

Chapter 5

Cellular Automata and Self-Organized Criticality

The notion of “phase transition” is a key concept in the theory of complex systems. Right at the point of a continuous transition between one phase and another, systems behave in a very special fashion; they are said to be “critical”. Criticality is reached normally when tuning an external parameter, such as the temperature for physical phase transitions.

The central question discussed in this chapter is whether “self-organized criticality” is possible in complex adaptive systems, i.e. whether a system can autonomously adapt its own parameters in a way to move towards criticality on its own, as a consequence of a suitable adaptive dynamics. Possible self-organized states in nature involve life as it is, where one speaks of “life at the edge of chaos”, and the neural dynamics of the human brain.

We will introduce in this chapter the Landau theory of phase transitions and then discuss cellular automata, an important and popular class of standardized dynamical systems. Cellular automata allow a very intuitive construction of models, such as the forest fire model, the game of life and the sandpile model, which exhibits self-organized criticality. The chapter then concludes with a discussion of whether self-organized criticality occurs in the most adaptive dynamical system of all, namely in the context of long-term evolution.

5.1 The Landau Theory of Phase Transitions

One may describe the physics of thermodynamic phases either microscopically with the tools of statistical physics, or by considering the general properties close to a phase transition. The Landau theory of phase transitions does the latter, providing a general framework valid irrespectively of the microscopic details of the material.

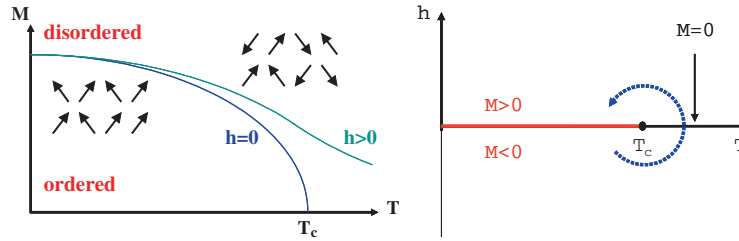


Fig. 5.1 Phase diagram of a magnet in an external magnetic field h . *Left*: The order parameter M (magnetization) as a function of temperature across the phase transition. The *arrows* illustrate typical arrangements of the local moments. In the ordered phase there is a net magnetic moment (magnetization). For $h = 0/h > 0$ the transition disorder-order is a sharp transition/crossover. *Right*: The $T - h$ phase diagram. A sharp transition occurs only for vanishing external field h

Second-Order Phase Transitions Phase transitions occur in many physical systems when the number of components diverges, viz “macroscopic” systems. Every phase has characteristic properties. The key property, which distinguishes one phase from another, is denoted the “order parameter”. Mathematically one can classify the type of ordering according to the symmetry of the ordering breaks.

The Order Parameter. In a continuous or “second-order” phase transition the high-temperature phase has a higher symmetry than the low-temperature phase and the degree of symmetry breaking can be characterized by an order parameter ϕ .

Note that all matter is disordered at high enough temperatures and ordered phases occur at low to moderate temperatures in physical systems.

Ferromagnetism in Iron The classical example for a phase transition is that of a magnet like iron. Above the Curie temperature of $T_c = 1,043$ K the elementary magnets are disordered, see Fig. 5.1 for an illustration. They fluctuate strongly and point in random directions. The net magnetic moment vanishes. Below the Curie temperature the moments point on the average to a certain direction creating such a macroscopic magnetic field. Since magnetic fields are generated by circulating currents and since an electric current depends on time, one speaks of a breaking of “time-reversal symmetry” in the magnetic state of a ferromagnet like iron. Some further examples of order parameters characterizing phase transitions in physical systems are listed in Table 5.1.

Free Energy A statistical mechanical system takes the configuration with the lowest energy at zero temperature. A physical system at finite temperatures $T > 0$ does not minimize its energy but a quantity called the *free energy*

F , which differs from the energy by a term proportional to the entropy and to the temperature.¹

Close to the transition temperature T_c the order parameter ϕ is small and one assumes within the Landau–Ginsburg model that the free energy density $f = F/V$,

$$f = f(T, \phi, h) ,$$

can be expanded for a small order parameter ϕ and a small external field h :

$$f(T, \phi, h) = f_0(T, h) - h\phi + a\phi^2 + b\phi^4 + \dots \quad (5.1)$$

where the parameters $a = a(T)$ and $b = b(T)$ are functions of the temperature T and of an external field h , e.g. a magnetic field for the case of magnetic systems. Note the linear coupling of the external field h to the order parameter in lowest order and that $b > 0$ (stability for large ϕ), compare Fig. 5.2.

Spontaneous Symmetry Breaking All odd terms $\sim \phi^{2n+1}$ vanish in the expansion (5.1). The reason is simple. The expression (5.1) is valid for all temperatures close to T_c and the disordered high-temperature state is invariant under the symmetry operation

$$f(T, \phi, h) = f(T, -\phi, -h), \quad \phi \leftrightarrow -\phi, \quad h \leftrightarrow -h .$$

This relation must therefore hold also for the exact Landau–Ginsburg functional. When the temperature is lowered the order parameter ϕ will acquire a finite expectation value. One speaks of a “spontaneous” breaking of the symmetry inherent to the system.

The Variational Approach The Landau–Ginsburg functional (5.1) expresses the value that the free-energy would have for all possible values of ϕ . The true physical state, which one calls the “thermodynamical stable state”, is obtained by finding the minimal $f(T, \phi, h)$ for all possible

¹ Details can be found in any book on thermodynamics and phase transitions, e.g. Callen (1985), they are, however, not necessary for an understanding of the following discussions.

Table 5.1 Examples of important types of phase transitions in physical systems. When the transition is continuous/discontinuous one speaks of a second-/first-order phase transition. Note that most order parameters are non-intuitive. The superconducting state, notable for its ability to carry electrical current without dispersion, breaks what one calls the $U(1)$ -gauge invariance of the normal (non-superconducting) metallic state

Transition	Type	Order parameter ϕ
Superconductivity	Second-order	$U(1)$ -gauge
Magnetism	Mostly second-order	Magnetization
Ferroelectricum	Mostly second-order	Polarization
Bose–Einstein	Second-order	Amplitude of $k = 0$ state
Liquid–gas	First-order	Density

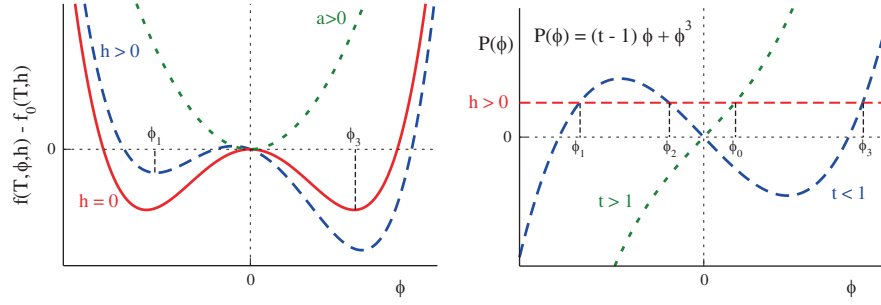


Fig. 5.2 *Left:* The functional dependence of the Landau–Ginzburg free energy $f(T, \phi, h) - f_0(T, h) = -h\phi + a\phi^2 + b\phi^4$, with $a = (t - 1)/2$. Plotted is the free energy for $a < 0$ and $h > 0$ (dashed line) and $h = 0$ (full line) and for $a > 0$ (dotted line). *Right:* Graphical solution of Eq. (5.9) for a non-vanishing field $h \neq 0$; ϕ_0 is the order parameter in the disordered phase ($t > 1$, dotted line), ϕ_1, ϕ_3 the stable solutions in the order phase ($t < 1$, dashed line) and ϕ_2 the unstable solution, compare the left-hand side illustration

values of ϕ :

$$\begin{aligned} \delta f &= (-h + 2a\phi + 4b\phi^3) \delta\phi = 0, \\ 0 &= -h + 2a\phi + 4b\phi^3, \end{aligned} \quad (5.2)$$

where δf and $\delta\phi$ denote small variations of the free energy and of the order parameter, respectively. This solution corresponds to a minimum in the free energy if

$$\delta^2 f > 0, \quad \delta^2 f = (2a + 12b\phi^2) (\delta\phi)^2. \quad (5.3)$$

One also says that the solution is “locally stable”, since any change in ϕ from its optimal value would raise the free energy.

Solutions for $h = 0$ We consider first the case with no external field, $h = 0$. The solution of Eq. (5.2) is then

$$\phi = \begin{cases} 0 & \text{for } a > 0 \\ \pm\sqrt{-a/(2b)} & \text{for } a < 0 \end{cases}. \quad (5.4)$$

The trivial solution $\phi = 0$ is stable,

$$(\delta^2 f)_{\phi=0} = 2a (\delta\phi)^2, \quad (5.5)$$

if $a > 0$. The nontrivial solutions $\phi = \pm\sqrt{-a/(2b)}$ of Eq. (5.4) are stable,

$$(\delta^2 f)_{\phi \neq 0} = -4a (\delta\phi)^2, \quad (5.6)$$

for $a < 0$. Graphically this is immediately evident, see Fig. 5.2. For $a > 0$ there is a single global minimum at $\phi = 0$, for $a < 0$ we have two symmetric minima.

Continuous Phase Transition We therefore find that the Ginsburg–Landau functional (5.1) describes continuous phase transitions when $a = a(T)$ changes sign at the critical temperature T_c . Expanding $a(T)$ for small $T - T_c$ we have

$$a(T) \sim T - T_c, \quad a = a_0(t - 1), \quad t = T/T_c, \quad a_0 > 0,$$

where we have used $a(T_c) = 0$. For $T < T_c$ (ordered phase) the solution Eq. (5.4) then takes the form

$$\phi = \pm \sqrt{\frac{a_0}{2b}}(1 - t), \quad t < 1, \quad T < T_c. \quad (5.7)$$

Simplification by Rescaling We can always rescale the order parameter ϕ , the external field h and the free energy density f such that $a_0 = 1/2$ and $b = 1/4$. We then have

$$a = \frac{t - 1}{2}, \quad f(T, \phi, h) - f_0(T, h) = -h\phi + \frac{t - 1}{2}\phi^2 + \frac{1}{4}\phi^4$$

and

$$\phi = \pm\sqrt{1 - t}, \quad t = T/T_c \quad (5.8)$$

for the non-trivial solution Eq. (5.7).

Solutions for $h \neq 0$ The solutions of Eq. (5.2) are determined in rescaled form by

$$h = (t - 1)\phi + \phi^3 \equiv P(\phi), \quad (5.9)$$

see Fig. 5.2. In general one finds three solutions $\phi_1 < \phi_2 < \phi_3$. One can show (see the Exercises) that the intermediate solution is always locally unstable and that ϕ_3 (ϕ_1) is globally stable for $h > 0$ ($h < 0$).

First-Order Phase Transition We note, see Fig. 5.2, that the solution ϕ_3 for $h > 0$ remains locally stable when we vary the external field slowly (adiabatically)

$$(h > 0) \rightarrow (h = 0) \rightarrow (h < 0)$$

in the ordered state $T < T_c$. At a certain critical field, see Fig. 5.3, the order parameter changes sign abruptly, jumping from the branch corresponding to $\phi_3 > 0$ to the branch $\phi_1 < 0$. One speaks of hysteresis, a phenomenon typical for first-order phase transitions.

Susceptibility When the system is disordered and approaches the phase transition from above, it has an increased sensitivity towards ordering under the influence of an external field h .

Susceptibility. The susceptibility χ of a system denotes its response to an external field:

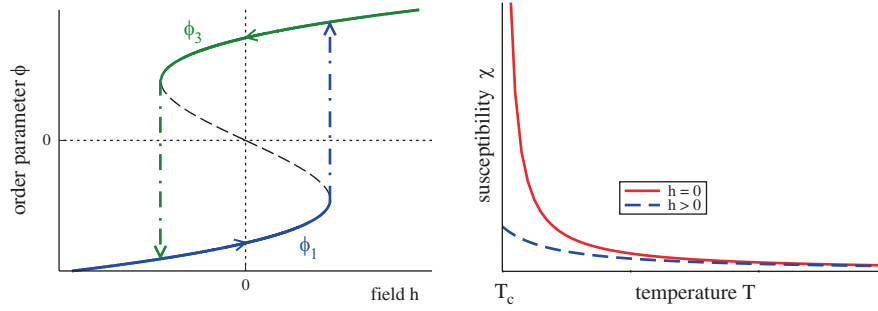


Fig. 5.3 *Left:* Discontinuous phase transition and hysteresis in the Landau model. Plotted is the solution $\phi = \phi(h)$ of $h = (t - 1)\phi + \phi^3$ in the ordered phase ($t < 1$) when changing the field h . *Right:* The susceptibility $\chi = \partial\phi/\partial h$ for $h = 0$ (solid line) and $h > 0$ (dotted line). The susceptibility divergence in the absence of an external field ($h = 0$), compare Eq. (5.11)

$$\chi = \left(\frac{\partial\phi}{\partial h} \right)_T, \quad (5.10)$$

where the subscript T indicates that the temperature is kept constant. The susceptibility measures the relative amount of the induced order $\phi = \phi(h)$.

Diverging Response Taking the derivative with respect to the external field h in Eq. (5.9), $h = (t - 1)\phi + \phi^3$, we find for the disordered phase $T > T_c$,

$$1 = \left[(t - 1) + 3\phi^2 \right] \frac{\partial\phi}{\partial h}, \quad \chi(T) \Big|_{h \rightarrow 0} = \frac{1}{t - 1} = \frac{T_c}{T - T_c}, \quad (5.11)$$

since $\phi(h = 0) = 0$ for $T > T_c$. The susceptibility diverges at the phase transition for $h = 0$, see Fig. 5.3. This divergence is a typical precursor of ordering for a second-order phase transition. Exactly at T_c , viz at criticality, the response of the system is, strictly speaking, infinite.

A non-vanishing external field $h \neq 0$ induces a finite amount of ordering $\phi \neq 0$ at all temperatures and the phase transition is masked, compare Fig. 5.1. In this case, the susceptibility is a smooth function of the temperature, see Eq. (5.11) and Fig. 5.3.

5.2 Criticality in Dynamical Systems

Length Scales Any physical or complex system normally has well defined time and space scales. As an example we take a look at the Schrödinger equation for the hydrogen atom,

$$i\hbar \frac{\partial \Psi(t, \mathbf{r})}{\partial t} = H \Psi(t, \mathbf{r}), \quad H = -\frac{\hbar^2 \Delta}{2m} - \frac{Ze^2}{|\mathbf{r}|},$$

where

$$\Delta = \frac{\partial^2}{\partial x^2} + \frac{\partial^2}{\partial y^2} + \frac{\partial^2}{\partial z^2}$$

is the Laplace operator. We do not need to know the physical significance of the parameters to realize that we can rewrite the differential operator H , called the ‘‘Hamilton’’ operator, as

$$H = -E_R \left(a_0^2 \Delta + \frac{2a_0}{|\mathbf{r}|} \right), \quad E_R = \frac{mZ^2 e^4}{2\hbar^2}, \quad a_0 = \frac{\hbar^2}{mZe^2}.$$

The length scale $a_0 = 0.53 \text{ \AA}/Z$ is called the ‘‘Bohr radius’’ and the energy scale $E_R = 13.6 \text{ eV}$ the ‘‘Rydberg energy’’, which corresponds to a frequency scale of $E_R/\hbar = 3.39 \cdot 10^{15} \text{ Hz}$. The energy scale E_R determines the ground state energy and the characteristic excitation energies. The length scale a_0 determines the mean radius of the ground state wavefunction and all other radius-dependent properties.

Similar length scales can be defined for essentially all dynamical systems defined by a set of differential equations. The damped harmonic oscillator and the diffusion equations, e.g. are given by

$$\ddot{x}(t) - \gamma \dot{x}(t) + \omega^2 x(t) = 0, \quad \frac{\partial \rho(t, \mathbf{r})}{\partial t} = D \Delta \rho(t, \mathbf{r}). \quad (5.12)$$

The parameters $1/\gamma$ and $1/\omega$, respectively, determine the time scales for relaxation and oscillation, and D is the diffusion constant.

Correlation Function A suitable quantity to measure and discuss the properties of the solutions of dynamical systems like the ones defined by Eq. (5.12) is the equal-time correlation function $S(r)$, which is the expectation value

$$S(r) = \langle \rho(t_0, \mathbf{x}) \rho(t_0, \mathbf{y}) \rangle, \quad r = |\mathbf{x} - \mathbf{y}|. \quad (5.13)$$

Here $\rho(t_0, \mathbf{x})$ denotes the particle density, for the case of the diffusion equation or when considering a statistical mechanical system of interacting particles. The exact expression for $\rho(t_0, \mathbf{x})$ in general depends on the type of dynamical system considered; for the Schrödinger equation $\rho(t, \mathbf{x}) = \Psi^*(t, \mathbf{x})\Psi(t, \mathbf{x})$, i.e. the probability to find the particle at time t at the point \mathbf{x} .

The equal-time correlation function then measures the probability to find a particle at position \mathbf{x} when there is one at \mathbf{y} . $S(r)$ is directly measurable in scattering experiments and therefore a key quantity for the characterization of a physical system. Often one is interested in the deviation of the correlation from the average behaviour. In this case one considers $\langle \rho(\mathbf{x}) \rho(\mathbf{y}) \rangle - \langle \rho(\mathbf{x}) \rangle \langle \rho(\mathbf{y}) \rangle$ for the correlation function $S(r)$.

Correlation Length Of interest is the behavior of the equal-time correlation function $S(r)$ for large distances $r \rightarrow \infty$. In general we have two possibilities:

$$S(r) \Big|_{r \rightarrow \infty} \sim \begin{cases} e^{-r/\xi} & \text{non-critical} \\ 1/r^{d-2+\eta} & \text{critical} \end{cases} . \quad (5.14)$$

In any “normal” (non-critical) system, correlations over arbitrary large distances cannot be built up, and the correlation function decays exponentially with the “correlation” length ξ . The notation $d - 2 + \eta > 0$ for the decay exponent of the critical system is a convention from statistical physics, where $d = 1, 2, 3, \dots$ is the dimensionality of the system.

Scale-Invariance and Self-Similarity If a control parameter, often the temperature, of a physical system is tuned such that it sits exactly at the point of a phase transition, the system is said to be critical. At this point there are no characteristic length scales.

Scale Invariance. If a measurable quantity, like the correlation function, decays like a power of the distance $\sim (1/r)^\delta$, with a critical exponent δ , the system is said to be critical or scale-invariant.

Power laws have no scale; they are self-similar,

$$S(r) = c_0 \left(\frac{r_0}{r}\right)^\delta \equiv c_1 \left(\frac{r_1}{r}\right)^\delta, \quad c_0 r_0^\delta = c_1 r_1^\delta,$$

for arbitrary distances r_0 and r_1 .

Universality at the Critical Point The equal-time correlation function $S(r)$ is scale-invariant at criticality, compare Eq. (5.14). This is a surprising statement, since we have seen before that the differential equations determining the dynamical system have well defined time and length scales. How then does the solution of a dynamical system become effectively independent of the parameters entering its governing equations?

Scale invariance implies that fluctuations occur over all length scales, albeit with varying probabilities. This can be seen by observing snapshots of statistical mechanical simulations of simple models, compare Fig. 5.4. The scale invariance of the correlation function at criticality is a central result of the theory of phase transitions and statistical physics. The properties of systems close to a phase transition are not determined by the exact values of their parameters, but by the structure of the governing equations and their symmetries. This circumstance is denoted “universality” and constitutes one of the reasons for classifying phase transitions according to the symmetry of their order parameters, see Table 5.1.

Autocorrelation Function The equal-time correlation function $S(r)$ measures real-space correlations. The corresponding quantity in the time domain is the autocorrelation function

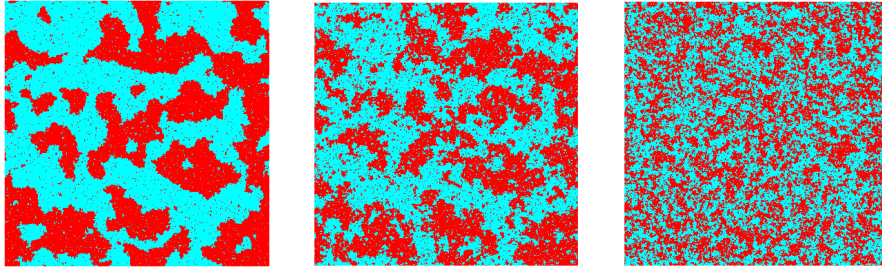


Fig. 5.4 Simulation of the 2D-Ising model $H = \sum_{\langle i,j \rangle} \sigma_i \sigma_j$, $\langle i,j \rangle$ nearest neighbors on a square lattice. Two magnetization orientations $\sigma_i = \pm 1$ correspond to the *dark/light dots*. For $T < T_c$ (*left, ordered*), $T \approx T_c$ (*middle, critical*) and $T > T_c$ (*right, disordered*). Note the occurrence of fluctuations at all length scales at criticality (self-similarity)

$$\Gamma(t) = \frac{\langle A(t+t_0)A(t_0) \rangle - \langle A \rangle^2}{\langle A^2 \rangle - \langle A \rangle^2}, \quad (5.15)$$

which can be defined for any time-dependent measurable quantity A , e.g. $A(t) = \rho(t, \vec{r})$. Note that the autocorrelations are defined relative to $\langle A \rangle^2$, viz the mean (time-independent) fluctuations. The denominator in Eq. (5.15) is a normalization convention, namely $\Gamma(0) \equiv 1$.

In the non-critical regime, viz the diffusive regime, no long-term memory is present in the system and all information about the initial state is lost exponentially,

$$\Gamma(t) \sim e^{-t/\tau}, \quad t \rightarrow \infty. \quad (5.16)$$

τ is called the relaxation time. The relaxation or autocorrelation time τ is the time scale of diffusion processes.

Dynamical Critical Exponent The relaxation time entering Eq. (5.16) diverges at criticality, as does the real-space correlation length ξ entering Eq. (5.14). One can then define an appropriate exponent z , dubbed the “dynamical critical exponent” z , in order to relate the two power laws for τ and ξ via

$$\tau \sim \xi^z, \quad \text{for} \quad \xi = |T - T_c|^{-\nu} \rightarrow \infty.$$

The autocorrelation time is divergent in the critical state $T \rightarrow T_c$.

Self-Organized Criticality We have seen that phase transitions can be characterized by a set of exponents describing the respective power laws of various quantities like the correlation function or the autocorrelation function. The phase transition occurs generally at a single point, viz $T = T_c$ for a thermodynamical system. At the phase transition the system becomes effectively independent of the details of its governing equations, being determined by symmetries.

It then comes as a surprise that there should exist complex dynamical systems that attain a critical state for a finite range of parameters. This

possibility, denoted “self-organized criticality” and the central subject of this chapter, is to some extent counter intuitive. We can regard the parameters entering the evolution equation as given externally. Self-organized criticality then signifies that the system effectively adapts to changes in the external parameters, e.g. to changes in the given time and length scales, in such a way that the stationary state becomes independent of those changes.

5.2.1 $1/f$ Noise

So far we have discussed the occurrence of critical states in classical thermodynamics and statistical physics. We now ask ourselves for experimental evidence that criticality might play a central role in certain time-dependent phenomena.

$1/f$ Noise The power spectrum of the noise generated by many real-world dynamical processes falls off inversely with frequency f . This $1/f$ noise has been observed for various biological activities, like the heart beat rhythms, for functioning electrical devices or for meteorological data series. Per Bak and coworkers have pointed out that the ubiquitous $1/f$ noise could be the result of a self-organized phenomenon. Within this view one may describe the noise as being generated by a continuum of weakly coupled damped oscillators representing the environment.

Power Spectrum of a Single Damped Oscillator A system with a single relaxation time τ , see Eq. (5.12), and eigenfrequency ω_0 has a Lorentzian power spectrum

$$S(\omega, \tau) = \operatorname{Re} \int_0^\infty dt e^{i\omega t} e^{-i\omega_0 t - t/\tau} = \operatorname{Re} \frac{-1}{i(\omega - \omega_0) - 1/\tau} = \frac{\tau}{1 + \tau^2(\omega - \omega_0)^2} .$$

For large frequencies $\omega \gg 1/\tau$ the power spectrum falls off like $1/\omega^2$. Being interested in the large- f behavior we will neglect ω_0 in the following.

Distribution of Oscillators The combined power or frequency spectrum of a continuum of oscillators is determined by the distribution $D(\tau)$ of relaxation times τ . For a critical system relaxation occurs over all time scales, as discussed in Sect. 5.2 and we may assume a scale-invariant distribution

$$D(\tau) \approx \frac{1}{\tau^\alpha} \quad (5.17)$$

for the relaxation times τ . This distribution of relaxation times yields a frequency spectrum

$$S(\omega) = \int d\tau D(\tau) \frac{\tau}{1 + (\tau\omega)^2} \sim \int d\tau \frac{\tau^{1-\alpha}}{1 + (\tau\omega)^2}$$

$$= \frac{1}{\omega \omega^{1-\alpha}} \int d(\omega\tau) \frac{(\omega\tau)^{1-\alpha}}{1 + (\tau\omega)^2} \sim \omega^{\alpha-2} . \quad (5.18)$$

For $\alpha = 1$ we obtain $1/\omega$, the typical behavior of $1/f$ noise.

The question is then how assumption (5.17) can be justified. The widespread appearance of $1/f$ noise can only happen when scale-invariant distribution of relaxation times are ubiquitous, viz if they were self-organized. The $1/f$ noise therefore constitutes an interesting motivation for the search of possible mechanisms leading to self-organized criticality.

5.3 Cellular Automata

Cellular automata are finite state lattice systems with discrete local update rules.

$$z_i \rightarrow f_i(z_i, z_{i+\delta}, \dots), \quad z_i \in [0, 1, \dots, n] , \quad (5.19)$$

where $i + \delta$ denote neighboring sites of site i . Each site or “cell” of the lattice follows a prescribed rule evolving in discrete time steps. At each step the new value for a cell depends only on the current state of itself and on the state of its neighbors.

Cellular automata differ from the dynamical networks we studied in Chap. ??, in two aspects:

- (i) The update functions are all identical: $f_i() \equiv f()$, viz they are translational invariant.
- (ii) The number n of states per cell is usually larger than 2 (boolean case).

Cellular automata can give rise to extremely complex behavior despite their deceptively simple dynamical structure. We note that cellular automata are always updated synchronously and never sequentially or randomly. The state of all cells is updated simultaneously.

Number of Update Rules The number of possible update rules is huge. Take, e.g. a two-dimensional model (square lattice), where each cell can take only one of two possible states,

$$z_i = 0, \quad (\text{dead}), \quad z_i = 1, \quad (\text{alive}) .$$

We consider, for simplicity, rules for which the evolution of a given cell to the next time step depends on the current state of the cell and on the values of each of its eight nearest neighbors. In this case there are

$$2^9 = 512 \text{ configurations}, \quad 2^{512} = 1.3 \times 10^{154} \text{ possible rules} ,$$

since any one of the 512 configurations can be mapped independently to “live” or “dead”. For comparison note that the universe is only of the order of 3×10^{17} seconds old.

Totalistic Update Rules It clearly does not make sense to explore systematically the consequences of arbitrary updating rules. One simplification is to consider a mean-field approximation that results in a subset of rules called “totalistic”.

For mean-field rules the new state of a cell depends only on the total number of living neighbors and on its own state. The eight-cell neighborhood has

$$9 \text{ possible total occupancy states of neighboring sites,} \\ 2 \cdot 9 = 18 \text{ configurations,} \quad 2^{18} = 262,144 \text{ totalistic rules .}$$

This is a large number, but it is exponentially smaller than the number of all possible update rules for the same neighborhood.

5.3.1 Conway’s Game of Life

The “game of life” takes its name because it attempts to simulate the reproductive cycle of a species. It is formulated on a square lattice and the update rule involves the eight-cell neighborhood. A new offspring needs exactly three parents in its neighborhood. A living cell dies of loneliness if it has less than two live neighbors, and of overcrowding if it has more than three live neighbors. A living cell feels comfortable with two or three live neighbors; in this case it survives. The complete set of updating rules is listed in Table 5.2.

Living Isolated Sets The time evolution of an initial set of a cluster of living cells can show extremely varied types of behavior. Fixpoints of the updating rules, such as a square

Table 5.2 Updating rules for the game of life; $z_i = 0, 1$ corresponds to empty and living cells. An “x” as an entry denotes what is going to happen for the respective number of living neighbors

		Number of living neighbors						
$z_i(t)$	$z_i(t+1)$	0	1	2	3	4	..	8
0	1					x		
	0	x	x	x	x			
1	1				x	x		
	0	x	x					x

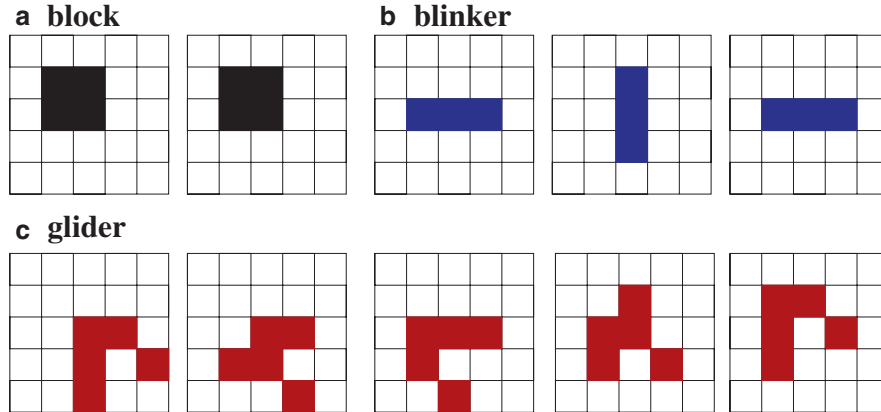


Fig. 5.5 Time evolution of some living configurations for the game of life, see Table 5.2. (a) The “block”; it quietly survives. (b) The “blinker”; it oscillates with period 2. (c) The “glider”; it shifts by $(-1, 1)$ after four time steps

$$\{(0, 0), (1, 0), (0, 1), (1, 1)\}$$

of four neighboring live cells, survive unaltered. There are many configurations of living cells which oscillate, such as three live cells in a row or column,

$$\{(-1, 0), (0, 0), (1, 0)\}, \quad \{(0, -1), (0, 0), (0, 1)\}.$$

It constitutes a fixpoint of $f(f(\cdot))$, alternating between a vertical and a horizontal bar. The configuration

$$\{(0, 0), (0, 1), (0, 2), (1, 2), (2, 1)\}$$

is dubbed “glider”, since it returns to its initial shape after four time steps but is displaced by $(-1, 1)$, see Fig. 5.5. It constitutes a fixpoint of $f(f(f(f(\cdot))))$ times the translation by $(-1, 1)$. The glider continues to propagate until it encounters a cluster of other living cells.

The Game of Life as a Universal Computer It is interesting to investigate, from an engineering point of view, all possible interactions between initially distinct sets of living cells in the game of life. In this context one finds that it is possible to employ gliders for the propagation of information over arbitrary distances. One can prove that arbitrary calculations can be performed by the game of life, when identifying the gliders with bits. Suitable and complicated initial configurations are necessary for this purpose, in addition to dedicated living subconfigurations performing logical computations, in analogy to electronic gates, when hit by one or more gliders.

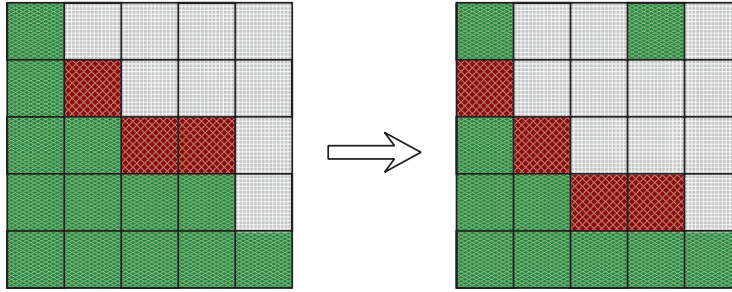


Fig. 5.6 Time evolution (from *left to right*) of a configuration of living trees (*green*), burning trees (*red*) and of places burnt down (*grey*), in the forest fire model. Places burnt down can regrow spontaneous with a small rate, the fire always spreads to nearest neighboring trees

5.3.2 The Forest Fire Model

The forest fires automaton is a very simplified model of real-world forest fires. It is formulated on a square lattice with three possible states per cell,

$$z_i = 0, \quad (\text{empty}), \quad z_i = 1, \quad (\text{tree}), \quad z_i = 2, \quad (\text{fire}).$$

A tree sapling can grow on every empty cell with probability $p < 1$. There is no need for nearby parent trees, as sperms are carried by wind over wide distances. Trees do not die in this model, but they catch fire from any burning nearest neighbor tree. The rules are illustrated in Fig. 5.6.

The forest fire automaton differs from typical rules, such as Conway's game of life, because it has a stochastic component. In order to have an interesting dynamics one needs to adjust the growth rate p as a function of system size, so as to keep the fire burning continuously. The fires burn down the whole forest when trees grow too fast. When the growth rate is too low, on the other hand, the fires, being surrounded by ashes, may die out completely.

$z_i(t)$	$z_i(t+1)$	Condition
Empty	Tree	With probability $p < 1$
Tree	Tree	No fire close by
Tree	Fire	At least one fire close by
Fire	Empty	Always

When adjusting the growth rate properly one reaches a steady state, the system having fire fronts continually sweeping through the forest, as is observed for real-world forest fires; this is illustrated in Fig. 5.7. In large systems stable spiral structures form and set up a steady rotation.

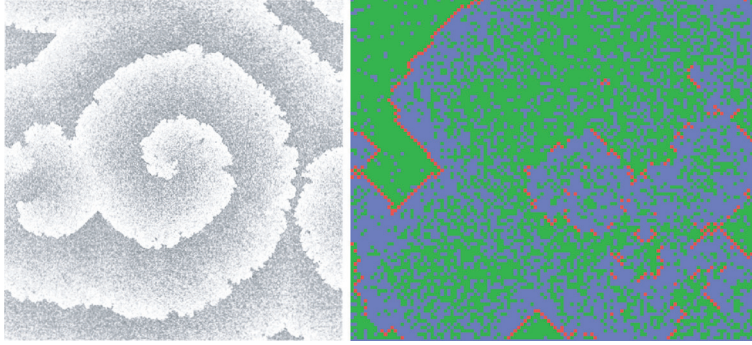


Fig. 5.7 Simulations of the forest fire model. *Left:* Fires burn in characteristic spirals for a growth probability $p = 0.005$ and no lightning, $f = 0$ (From [Clar et al. 1996](#)). *Right:* A snapshot of the forest fire model with a growth probability $p = 0.06$ and a lightning probability $f = 0.0001$. Note the characteristic fire fronts with trees in front and ashes behind

Criticality and Lightning The forest fire model, as defined above, is not critical, since the characteristic time scale $1/p$ for the regrowth of trees governs the dynamics. This time scale translates into a characteristic length scale $1/p$, which can be observed in [Fig. 5.7](#), via the propagation rule for the fire.

Self-organized criticality can, however, be induced in the forest fire model when introducing an additional rule, namely that a tree might ignite spontaneously with a small probability f , when struck by lightning, causing also small patches of forest to burn. We will not discuss this mechanism in detail here, treating instead in the next section the occurrence of self-organized criticality in the sandpile model on a firm mathematical basis.

5.4 The Sandpile Model and Self-Organized Criticality

Self-Organized Criticality We have learned in [Chap. ??](#) about the concept “life at the edge of chaos”. Namely, that certain dynamical and organizational aspects of living organisms may be critical. Normal physical and dynamical systems, however, show criticality only for selected parameters, e.g. $T = T_c$, see [Sect. 5.1](#). For criticality to be biologically relevant, the system must evolve into a critical state starting from a wide range of initial states – one speaks of “self-organized criticality”.

The Sandpile Model Per Bak and coworkers introduced a simple cellular automaton that mimics the properties of sandpiles, i.e. the BTW model. Every cell is characterized by a force

$$z_i = z(i, j) = 0, 1, 2, \dots, \quad i, j = 1, \dots, L$$

on a finite $L \times L$ lattice. There is no one-to-one correspondence of the sandpile model to real-world sandpiles. Loosely speaking one may identify the force z_i with the slope of real-world sandpiles. But this analogy is not rigorous, as the slope of a real-world sandpile is a continuous variable. The slopes belonging to two neighboring cells should therefore be similar, whereas the values of z_i and z_j on two neighboring cells can differ by an arbitrary amount within the sandpile model.

The sand begins to topple when the slope gets too big:

$$z_j \rightarrow z_j - \Delta_{ij}, \quad \text{if} \quad z_i > K ,$$

where K is the threshold slope and with the toppling matrix

$$\Delta_{i,j} = \begin{cases} 4 & i = j \\ -1 & i, j \text{ nearest neighbors} \\ 0 & \text{otherwise} \end{cases} . \quad (5.20)$$

This update rule is valid for the four-cell neighborhood $\{(0, \pm 1), (\pm 1, 0)\}$. The threshold K is arbitrary, a shift in K simply shifts z_i . It is customary to consider $K = 3$. Any initial random configuration will then relax into a steady-state final configuration (called the stable state) with

$$z_i = 0, 1, 2, 3, \quad (\text{stable state}) .$$

Open Boundary Conditions The update rule Eq. (5.20) is conserving:

Conserving Quantities. If there is a quantity that is not changed by the update rule it is said to be conserving.

The sandpile model is locally conserving. The total height $\sum_j z_j$ is constant due to $\sum_j \Delta_{i,j} = 0$. Globally, however, it is not conserving, as one uses open boundary conditions for which excess sand is lost at the boundary. When a site at the boundary topples, some sand is lost there and the total $\sum_j z_j$ is reduced by one.

However, here we have only a vague relation of the BTW model to real-world sandpiles. The conserving nature of the sandpile model mimics the fact that sand grains cannot be lost in real-world sandpiles. This interpretation, however, contrasts with the previously assumed correspondence of z_i with the slope of real-world sandpiles.

Avalanches When starting from a random initial state with $z_i \ll K$ the system settles in a stable configuration when adding “grains of sand” for a while. When a grain of sand is added to a site with $z_i = K$

$$z_i \rightarrow z_i + 1, \quad z_i = K ,$$

a toppling event is induced, which may in turn lead to a whole series of topplings. The resulting avalanche is characterized by its duration t and the

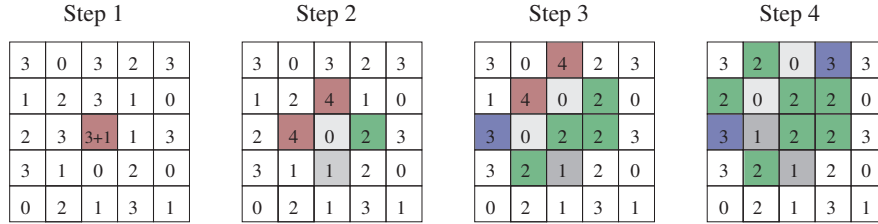


Fig. 5.8 The progress of an avalanche, with duration $t = 3$ and size $s = 13$, for a sandpile configuration on a 5×5 lattice with $K = 3$. The height of the sand in each cell is indicated by the numbers. The *shaded region* is where the avalanche has progressed. The avalanche stops after step 3

size s of affected sites. It continues until a new stable configuration is reached. In Fig. 5.8 a small avalanche is shown.

Distribution of Avalanches We define with $D(s)$ and $D(t)$ the distributions of the size and of the duration of avalanches. One finds that they are scale-free,

$$D(s) \sim s^{-\alpha_s}, \quad D(t) \sim t^{-\alpha_t}, \quad (5.21)$$

as we will discuss in the next section. Equation (5.21) expresses the essence of self-organized criticality. We expect these scale-free relations to be valid for a wide range of cellular automata with conserving dynamics, independent of the special values of the parameters entering the respective update functions. Numerical simulations and analytic approximations for $d = 2$ dimensions yield

$$\alpha_s \approx \frac{5}{4}, \quad \alpha_t \approx \frac{3}{4}.$$

Conserving Dynamics and Self-Organized Criticality We note that the toppling events of an avalanche are (locally) conserving. Avalanches of arbitrary large sizes must therefore occur, as sand can be lost only at the boundary of the system. One can indeed prove that Eqs. (5.21) are valid only for locally conserving models. Self-organized criticality breaks down as soon as there is a small but non-vanishing probability to lose sand somewhere inside the system.

Features of the Critical State The empty board, when all cells are initially empty, $z_i \equiv 0$, is not critical. The system remains in the frozen phase when adding sand; compare Chap. ??, as long as most $z_i < K$. Adding one sand corn after the other the critical state is slowly approached. There is no way to avoid the critical state.

Once the critical state is achieved the system remains critical. This critical state is paradoxically also the point at which the system is dynamically most unstable. It has an unlimited susceptibility to an external driving (adding a grain of sand), using the terminology of Sect. 5.1, as a single added grain of sand can trip avalanches of arbitrary size.

It needs to be noted that the dynamics of the sandpile model is deterministic, once the grain of sand has been added, and that the disparate fluctuations in terms of induced avalanches are features of the critical state per se and not due to any hidden stochasticity, as discussed in Chap. ??, or due to any hidden deterministic chaos.

5.4.1 Absorbing Phase Transitions

One can take away from the original sandpile model both the external drive, the adding of sand grains, and the dissipation. Instead of losing sand at the boundaries one then considers periodic boundary conditions and the number of grains is consequently conserved both locally as well as globally. Starting with a random configuration $\{z_i\}$ there will be a rush of initial avalanches, following the toppling rules (5.20), until the system settles into either an active or an absorbing state.

- All grain topplings will stop eventually whenever the average number of grains is too small. The resulting inactive configuration is called “absorbing state”.
- For a large average number of grains the redistribution of grains will never terminate, resulting in a continuously “active state”.

Adding externally a single grain to an absorbing state will lead generically only to a single avalanche with the transient activity terminating in another absorbing state. In this picture the grain of sand added has been absorbed.

Transition from Absorbing to Active State The average number of particles $\rho = \langle z_i \rangle$ controls the transition from absorbing to active state. The active state is characterized by the mean number κ of active states, which is the number of sites with heights z_i greater than the threshold K . The avalanche shown in Fig. 5.8, has, to give an example, 1/2/2/0 active sites respectively at time steps 1/2/3/4. The transition from the absorbing to the active state is of second order, as illustrated in Fig. 5.9, with κ acting as an order parameter.

Self-Organization Towards the Critical Density There is a deep relation between absorbing state transitions in general and the concept of self-organized criticality, based on a separation of time scales.

The external drive, the addition of grains of sand, one by one, is infinitesimal slow in the sandpile model. The reason being that the external drive is stopped once an avalanche starts, and resumed only once the avalanche has terminated. The avalanche is hence instantaneous, relative to the time scale of the external drive. Slowly adding one particle after another continuously increases the mean particle number and drives the system, from below, towards criticality, Fig. 5.8. Particles surpassing the critical density

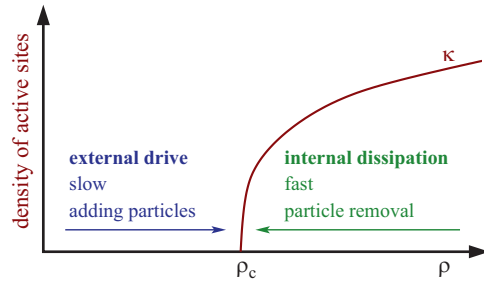


Fig. 5.9 Changing the mean particle density, ρ an absorbing phase transition may occur, with the density of active sites acting as an order parameter. The system may self-organize towards the critical particle density ρ_c through balancing of a slow external drive, realized by adding grains in the sandpile model, and a fast internal dissipative process, when losing grains of sand at the boundaries

are instantaneously dissipated through large avalanches reaching the boundaries of the systems, the mean particle density is hence pinned at criticality.

5.5 Random Branching Theory

Branching theory deals with the growth of networks via branching. Networks generated by branching processes are loopless; they typically arise in theories of evolutionary processes.

5.5.1 Branching Theory of Self-Organized Criticality

Avalanches have an intrinsic relation to branching processes: at every time step the avalanche can either continue or stop. Random branching theory is hence a suitable method for studying self-organized criticality.

Branching in Sandpiles A typical update during an avalanche is of the form

$$\begin{aligned} \text{time 0: } & z_i \rightarrow z_i - 4 & z_j & \rightarrow z_j + 1 \\ \text{time 1: } & z_i \rightarrow z_i + 1 & z_j & \rightarrow z_j - 4 \end{aligned}$$

when two neighboring cells i and j initially have $z_i = K + 1$ and $z_j = K$. This implies that an avalanche typically intersects with itself. Consider, however, a general d -dimensional lattice with $K = 2d - 1$. The self-interaction of the avalanche becomes unimportant in the limit $1/d \rightarrow 0$ and the avalanche can be mapped rigorously to a random branching process. Note that we encountered an analogous situation in the context of high-dimensional or random

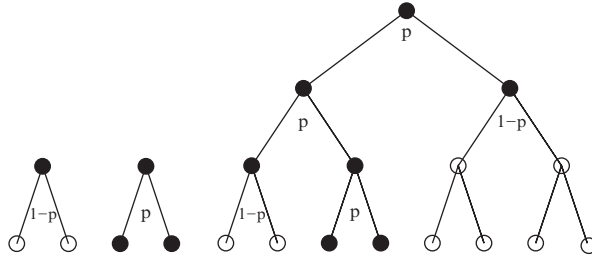


Fig. 5.10 Branching processes. *Left:* The two possible processes of order $n = 1$. *Right:* A generic process of order $n = 3$ with an avalanche of size $s = 7$

graphs, discussed in Chap. ??, which are also loopless in the thermodynamic limit.

Binary Random Branching In $d \rightarrow \infty$ the notion of neighbors loses meaning, avalanches then have no spatial structure. Every toppling event affects $2d$ neighbors, on a d -dimensional hypercubic lattice. However, only the cumulative probability of toppling of the affected cells is relevant, due to the absence of geometric constraints in the limit $d \rightarrow \infty$. All that is important then is the question whether an avalanche continues, increasing its size continuously, or whether it stops.

We can therefore consider the case of binary branching, viz that a toppling event creates two new active sites.

Binary Branching. An active site of an avalanche topples with the probability p and creates two new active sites.

For $p < 1/2$ the number of new active sites decreases on the average and the avalanche dies out. $p_c = 1/2$ is the critical state with (on the average) conserving dynamics. See Fig. 5.10 for some examples of branching processes.

Distribution of Avalanche Sizes The properties of avalanches are determined by the probability distribution,

$$P_n(s, p), \quad \sum_{s=1}^{\infty} P_n(s, p) = 1 ,$$

describing the probability to find an avalanche of size s in a branching process of order n . Here s is the (odd) number of sites inside the avalanche, see Figs. 5.10 and 5.11 for some examples.

Generating Function Formalism In Chap. ??, we introduced the generating functions for probability distribution. This formalism is very useful when one has to deal with independent stochastic processes, as the joint probability of two independent stochastic processes is equivalent to the simple multiplication of the corresponding generating functions.

We define via

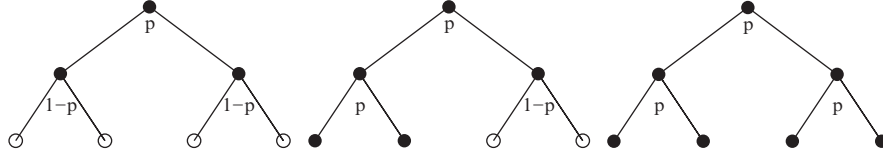


Fig. 5.11 Branching processes of order $n = 2$ with avalanches of sizes $s = 3, 5, 7$ (left, middle, right) and boundaries $\sigma = 0, 2, 4$

$$f_n(x, p) = \sum_s P_n(s, p) x^s, \quad f_n(1, p) = \sum_s P_n(s, p) = 1 \quad (5.22)$$

the generating functional $f_n(x, p)$ for the probability distribution $P_n(s, p)$. We note that

$$P_n(s, p) = \frac{1}{s!} \left. \frac{\partial^s f_n(x, p)}{\partial x^s} \right|_{x=0}, \quad n, p \text{ fixed} . \quad (5.23)$$

Small Avalanches For small s and large n one can evaluate the probability for small avalanches to occur by hand and one finds for the corresponding generating functionals:

$$P_n(1, p) = 1 - p, \quad P_n(3, p) = p(1 - p)^2, \quad P_n(5, p) = 2p^2(1 - p)^3 ,$$

compare Figs. 5.10 and 5.11. Note that $P_n(1, p)$ is the probability to find an avalanche of just one site.

The Recursion Relation For generic n the recursion relation

$$f_{n+1}(x, p) = x(1 - p) + xp f_n^2(x, p) \quad (5.24)$$

is valid. To see why, one considers building the branching network backwards, adding a site at the top:

- With the probability $(1 - p)$ one adds a single-site avalanche described by the generating functional x .
- With the probability p one adds a site, described by the generating functional x , which generated two active sites, described each by the generating functional $f_n(x, p)$.

In the terminology of branching theory, one also speaks of a decomposition of the branching process after its first generation, a standard procedure.

The Self-Consistency Condition For large n and finite x the generating functionals $f_n(x, p)$ and $f_{n+1}(x, p)$ become identical, leading to the self-consistency condition

$$f_n(x, p) = f_{n+1}(x, p) = x(1 - p) + xp f_n^2(x, p) , \quad (5.25)$$

with the solution

$$f(x, p) \equiv f_n(x, p) = \frac{1 - \sqrt{1 - 4x^2p(1-p)}}{2xp} \quad (5.26)$$

for the generating functional $f(x, p)$. The normalization condition

$$f(1, p) = \frac{1 - \sqrt{1 - 4^2p(1-p)}}{2p} = \frac{1 - \sqrt{(1-2p)^2}}{2p} = 1$$

is fulfilled for $p \in [0, 1/2]$. For $p > 1/2$ the last step in above equation would not be correct.

The Subcritical Solution Expanding Eq. (5.26) in powers of x^2 we find terms like

$$\frac{1}{p} [4p(1-p)]^k \frac{(x^2)^k}{x} = \frac{1}{p} [4p(1-p)]^k x^{2k-1} .$$

Comparing this with the definition of the generating functional Eq. (5.22) we note that $s = 2k - 1$, $k = (s + 1)/2$ and that

$$P(s, p) \sim \frac{1}{p} \sqrt{4p(1-p)} [4p(1-p)]^{s/2} \sim e^{-s/s_c(p)} , \quad (5.27)$$

where we have used the relation

$$a^{s/2} = e^{\ln(a^{s/2})} = e^{-s(\ln a)/(-2)} , \quad a = 4p(1-p) ,$$

and where we have defined the avalanche correlation size

$$s_c(p) = \frac{-2}{\ln[4p(1-p)]} , \quad \lim_{p \rightarrow 1/2} s_c(p) \rightarrow \infty .$$

For $p < 1/2$ the size correlation length $s_c(p)$ is finite and the avalanche is consequently not scale-free, see Sect. 5.2. The characteristic size of an avalanche $s_c(p)$ diverges for $p \rightarrow p_c = 1/2$. Note that $s_c(p) > 0$ for $p \in]0, 1[$.

The Critical Solution We now consider the critical case with

$$p = 1/2, \quad 4p(1-p) = 1, \quad f(x, p) = \frac{1 - \sqrt{1 - x^2}}{x} .$$

The expansion of $\sqrt{1 - x^2}$ with respect to x is

$$\sqrt{1 - x^2} = \sum_{k=0}^{\infty} \frac{\frac{1}{2} (\frac{1}{2} - 1) (\frac{1}{2} - 2) \cdots (\frac{1}{2} - k + 1)}{k!} (-x^2)^k$$

in Eq. (5.26) and therefore

$$P_c(k) \equiv P(s = 2k - 1, p = 1/2) = \frac{\frac{1}{2} (\frac{1}{2} - 1) (\frac{1}{2} - 2) \cdots (\frac{1}{2} - k + 1)}{-k!} (-1)^k .$$

This expression is still unhandy. We are, however, only interested in the asymptotic behavior for large avalanche sizes s . For this purpose we consider the recursive relation

$$P_c(k+1) = \frac{1/2 - k}{k+1}(-1)P_c(k) = \frac{1 - 1/(2k)}{1 + 1/k}P_c(k)$$

in the limit of large $k = (s+1)/2$, where $1/(1 + 1/k) \approx 1 - 1/k$,

$$P_c(k+1) \approx \left[1 - 1/(2k)\right] \left[1 - 1/k\right] P_c(k) \approx \left[1 - 3/(2k)\right] P_c(k) .$$

This asymptotic relation leads to

$$\frac{P_c(k+1) - P_c(k)}{1} = \frac{-3}{2k} P_c(k), \quad \frac{\partial P_c(k)}{\partial k} = \frac{-3}{2k} P_c(k) ,$$

with the solution

$$P_c(k) \sim k^{-3/2}, \quad D(s) = P_c(s) \sim s^{-3/2}, \quad \alpha_s = \frac{3}{2}, \quad (5.28)$$

for large k, s , since $s = 2k - 1$.

Distribution of Relaxation Times The distribution of the duration n of avalanches can be evaluated in a similar fashion. For this purpose one considers the probability distribution function

$$Q_n(\sigma, p)$$

for an avalanche of duration n to have σ cells at the boundary, see Fig. 5.11.

One can then derive a recursion relation analogous to Eq. (5.24) for the corresponding generating functional and solve it self-consistently. We leave this as an exercise for the reader.

The distribution of avalanche durations is then given by considering $Q_n = Q_n(\sigma = 0, p = 1/2)$, i.e. the probability that the avalanche stops after n steps. One finds

$$Q_n \sim n^{-2}, \quad D(t) \sim t^{-2}, \quad \alpha_t = 2 . \quad (5.29)$$

Tuned or Self-Organized Criticality? The random branching model discussed in this section had only one free parameter, the probability p . This model is critical only for $p \rightarrow p_c = 1/2$, giving rise to the impression that one has to fine tune the parameters in order to obtain criticality, just like in ordinary phase transitions.

This, however, is not the case. As an example we could generalize the sandpile model to continuous forces $z_i \in [0, \infty]$ and to the update rules

$$z_j \rightarrow z_j - \Delta_{ij}, \quad \text{if} \quad z_i > K ,$$

and

$$\Delta_{i,j} = \begin{cases} K & i = j \\ -cK/4 & i, j \text{ nearest neighbors} \\ -(1-c)K/8 & i, j \text{ next-nearest neighbors} \\ 0 & \text{otherwise} \end{cases} \quad (5.30)$$

for a square-lattice with four nearest neighbors and eight next-nearest neighbors (Manhattan distance). The update rules are conserving,

$$\sum_j \Delta_{ij} = 0, \quad \forall c \in [0, 1].$$

For $c = 1$ this model corresponds to the continuous field generalization of the BTW model. The model defined by Eqs. (5.30), which has not yet been studied in the literature, might be expected to map in the limit $d \rightarrow \infty$ to an appropriate random branching model with $p = p_c = 1/2$ and to be critical for all values of the parameters K and c , due to its conserving dynamics.

5.5.2 Galton-Watson Processes

Galton-Watson processes are generalizations of the binary branching processes considered so far, with interesting applications in evolution theory and some everyday experiences.

The History of Family Names Family names are handed down traditionally from father to son. Family names regularly die out, leading over the course of time to a substantial reduction of the pool of family names. This effect is especially pronounced in countries looking back on millenia of cultural continuity, like China, where 22% of the population are sharing only three family names.

The evolution of family names is described by a Galton-Watson process and a key quantity of interest is the extinction probability, viz the probability that the last person bearing a given family name dies without descendants.

The Galton-Watson Process The basic reproduction statistics determines the evolution of family names, see Fig. 5.12.

We denote with p_m the probability that an individual has m offsprings and with $G_0(x) = \sum_m p_m x^m$ its generating function. Defining with $p_m^{(n)}$ the probability of finding a total of m descendants in the n -th generation, we find the recursion relation

$$G^{(n+1)}(x) = \sum_m p_m^{(n)} [G_0(x)]^m = G^{(n)}(G_0(x)), \quad G^{(n)}(x) = \sum_m p_m^{(n)} x^m$$

for the respective generating function. Using the initial condition $G^{(0)}(x) = x$ we may rewrite this recursion relation as

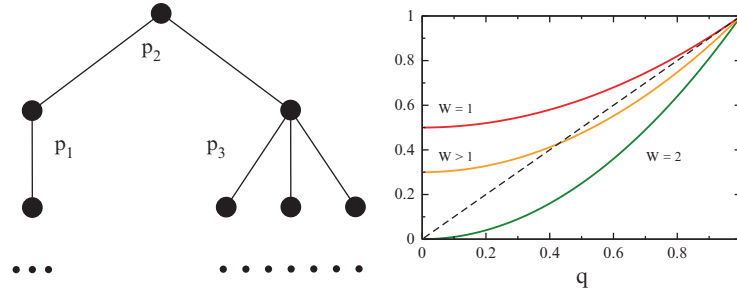


Fig. 5.12 Galton-Watson processes. *Left:* Example of a reproduction tree, p_m being the probabilities of having $m = 0, 1, \dots$ offsprings. *Right:* Graphical solution for the fixpoint equation (5.33), for various average numbers of offsprings W

$$G^{(n)}(x) = G_0(G_0(\dots G_0(x) \dots)) = G_0 \left(G^{(n-1)}(x) \right) . \quad (5.31)$$

This recursion relation is the basis for all further considerations; we consider here the extinction probability q .

Extinction Probability The reproduction process dies out when there is a generation with zero members. The probability of having zero persons bearing the given family name in the n -th generation is

$$q = p_0^{(n)} = G^{(n)}(0) = G_0 \left(G^{(n-1)}(0) \right) = G_0(q) , \quad (5.32)$$

where we have used the recursion relation Eq. (5.31) and the stationary condition $G^{(n)}(0) \approx G^{(n-1)}(0)$. The extinction probability q is hence given by the fixpoint $q = G_0(q)$ of the generating functional $G_0(x)$ of the reproduction probability.

Binary Branching as a Galton-Watson Process As an example we consider the case that

$$G_0(x) = 1 - \frac{W}{2} + \frac{W}{2}x^2, \quad G_0'(1) = W ,$$

viz that people may not have but either zero or two sons, with probabilities $1 - W/2$ and $W/2 < 1$ respectively. The expected number of offsprings W is also called the fitness in evolution theory, see Chap. ???. This setting corresponds to the case of binary branching, see Fig. 5.10, with $W/2$ being the branching probability, describing the reproductive dynamics of unicellular bacteria.

The self-consistency condition (5.32) for the extinction probability $q = q(W)$ then reads

$$q = 1 - \frac{W}{2} + \frac{W}{2}q^2, \quad q(W) = \frac{1}{W} \pm \sqrt{\frac{1}{W^2} - \frac{(2-W)^2}{W^2}} , \quad (5.33)$$

with the smaller root being here of relevance. The extinction probability vanishes for a reproduction rate of two,

$$q(W) = \begin{cases} 0 & W = 2 \\ q \in]0, 1[& 1 < W < 2 \\ 1 & W \leq 1 \end{cases}$$

and is unity for a fitness below one, compare Fig. 5.12.

5.6 Application to Long-Term Evolution

An application of the techniques developed in this chapter can be used to study a model for the evolution of species proposed by Bak and Sneppen.

Fitness Landscapes Evolution deals with the adaption of species and their fitness relative to the ecosystem they live in.

Fitness Landscapes. The function that determines the chances of survival of a species, its fitness, is called the fitness landscape.

In Fig. 5.13 a simple fitness landscape, in which there is only one dimension in the genotype (or phenotype)² space, is illustrated.

The population will spend most of its time in a local fitness maximum, whenever the mutation rate is low with respect to the selection rate, since there are fitness barriers, see Fig. 5.13, between adjacent local fitness maxima. Mutations are random processes and the evolution from one local fitness maximum to the next can then happen only through a stochastic escape, a process we discussed in Chap. ??.

Coevolution It is important to keep in mind for the following discussion that an ecosystem, and with it the respective fitness landscapes, is not static on long time scales. The ecosystem is the result of the combined action of geophysical factors, such as the average rainfall and temperature, and biological influences, viz the properties and actions of the other constituting species. The evolutionary progress of one species will therefore, in general, trigger adaption processes in other species appertaining to the same ecosystem, a process denoted “coevolution”.

Evolutionary Time Scales In the model of Bak and Sneppen there are no explicit fitness landscapes like the one illustrated in Fig. 5.13. Instead the model attempts to mimic the effects of fitness landscapes, viz the influence of all the other species making up the ecosystem, by a single number, the “fitness barrier”. The time needed for a stochastic escape from one local

² The term “genotype” denotes the ensemble of genes. The actual form of an organism, the “phenotype”, is determined by the genotype plus environmental factors, like food supply during growth.

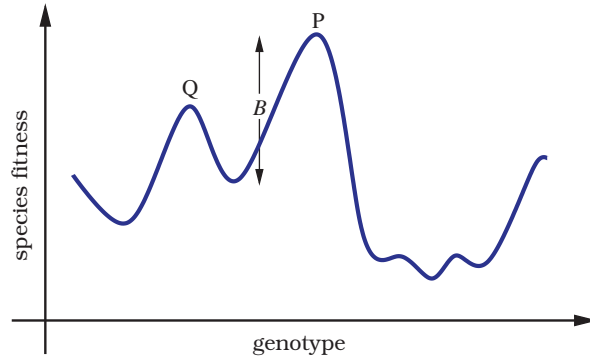


Fig. 5.13 Illustration of a one-dimensional fitness landscape. A species evolving from an adaptive peak P to a new adaptive peak Q needs to overcome the fitness barrier B

fitness optimum increases exponentially with the barrier height. We may therefore assume that the average time t it takes to mutate across a fitness barrier of height B scales as

$$t = t_0 e^{B/T}, \quad (5.34)$$

where t_0 and T are constants. The value of t_0 merely sets the time scale and is not important. The parameter T depends on the mutation rate, and the assumption that mutation is low implies that T is small compared with the typical barrier heights B in the landscape. In this case the time scales t for crossing slightly different barriers are distributed over many orders of magnitude and only the lowest barrier is relevant.

The Bak and Sneppen Model The Bak and Sneppen model is a phenomenological model for the evolution of barrier heights. The number N of species is fixed and each species has a respective barrier

$$B_i = B_i(t) \in [0, 1], \quad t = 0, 1, 2, \dots$$

for its further evolution. The initial $B_i(0)$ are drawn randomly from $[0, 1]$. The model then consists of the repetition of two steps:

1. The times for a stochastic escape are exponentially distributed, see Eq. (5.34). It is therefore reasonable to assume that the species with the lowest barrier B_i mutates and escapes first. After escaping, it will adapt quickly to a new local fitness maximum. At this point it will then have a new barrier for mutation, which is assumed to be uniformly distributed in $[0, 1]$.
2. The fitness function for a species i is given by the ecological environment it lives in, which is made up of all the other species. When any given species mutates it therefore influences the fitness landscape for a certain number

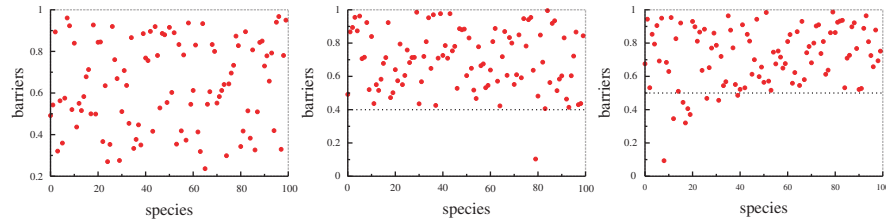


Fig. 5.14 The barrier values (*dots*) for a 100 species one-dimensional Bak–Sneppen model after 50, 200 and 1,600 steps of a simulation. The *horizontal line* in each frame represents the approximate position of the upper edge of the “gap”. A few species have barriers below this level, indicating that they were involved in an avalanche at the moment when the snapshot of the system was taken

of other species. Within the Bak and Sneppen model this translates into assigning new random barriers B_j for $K - 1$ neighbors of the mutating species i .

The Bak and Sneppen model therefore tries to capture two essential ingredients of long-term evolution: The exponential distribution of successful mutations and the interaction of species via the change of the overall ecosystem, when one constituting species evolves.

The Random Neighbor Model The topology of the interaction between species in the Bak–Sneppen model is unclear. It might be chosen as two-dimensional, if the species are thought to live geographically separated, or one-dimensional in a toy model. In reality the topology is complex and can be assumed to be, in first approximation, random, resulting in the soluble random neighbor model.

Evolution of Barrier Distribution Let us discuss qualitatively the redistribution of barrier heights under the dynamics, the sequential repetition of steps (1) and (2) above, see Fig. 5.14. The initial barrier heights are uniformly distributed over the interval $[0, 1]$ and the lowest barrier, removed in step (1), is small. The new heights reassigned in steps (1) and (2) will therefore lead, on the average, to an increase of the average barrier height with passing time.

With increasing average barrier height the characteristic lowest barrier is also raised and eventually a steady state will be reached, just as in the sand-pile model discussed previously. It turns out that the characteristic value for the lowest barrier is about $1/K$ at equilibrium in the mean-field approximation and that the steady state is critical.

Molecular Field Theory In order to solve the Bak–Sneppen model, we define the barrier distribution function,

$$p(x, t) ,$$

viz the probability to find a barrier of height $x \in [0, 1]$ at time step $t = 1, 2, \dots$. In addition, we define with $Q(x)$ the probability to find a barrier above x :

$$Q(x) = \int_x^1 dx' p(x'), \quad Q(0) = 1, \quad Q(1) = 0. \quad (5.35)$$

The dynamics is governed by the size of the smallest barrier. The distribution function $p_1(x)$ for the lowest barrier is

$$p_1(x) = N p(x) Q^{N-1}(x), \quad (5.36)$$

given by the probability $p(x)$ for one barrier (out of the N barriers) to have the barrier height x , while all the other $N - 1$ barriers are larger. $p_1(x)$ is normalized,

$$\int_0^1 dx p_1(x) = (-N) \int_0^1 dx Q^{N-1}(x) \frac{\partial Q(x)}{\partial x} = -Q^N(x) \Big|_{x=0}^{x=1} = 1,$$

where we used $p(x) = -Q'(x)$, $Q(0) = 1$ and $Q(1) = 0$, see Eq. (5.35).

Time Evolution of Barrier Distribution The time evolution for the barrier distribution consists in taking away one (out of N) barrier, the lowest, via

$$p(x, t) - \frac{1}{N} p_1(x, t),$$

and by removing randomly $K - 1$ barriers from the remaining $N - 1$ barriers, and adding K random barriers:

$$\begin{aligned} p(x, t+1) &= p(x, t) - \frac{1}{N} p_1(x, t) \\ &\quad - \frac{K-1}{N-1} \left(p(x, t) - \frac{1}{N} p_1(x, t) \right) + \frac{K}{N}. \end{aligned} \quad (5.37)$$

We note that $p(x, t+1)$ is normalized whenever $p(x, t)$ and $p_1(x, t)$ were normalized correctly:

$$\begin{aligned} \int_0^1 dx p(x, t+1) &= 1 - \frac{1}{N} - \frac{K-1}{N-1} \left(1 - \frac{1}{N} \right) + \frac{K}{N} \\ &= \left(1 - \frac{K-1}{N-1} \right) \frac{N-1}{N} + \frac{K}{N} = \frac{N-K}{N} + \frac{K}{N} \equiv 1. \end{aligned}$$

Stationary Distribution After many iterations of Eq. (5.37) the barrier distribution will approach a stationary solution $p(x, t+1) = p(x, t) \equiv p(x)$, as can be observed from the numerical simulation shown in Fig. 5.14. The stationary distribution corresponds to the fixpoint condition

$$0 = p_1(x) \frac{1}{N} \left(\frac{K-1}{N-1} - 1 \right) - p(x) \frac{K-1}{N-1} + \frac{K}{N}$$

of Eq. (5.37). Using the expression $p_1 = NpQ^{N-1}$, see Eq. (5.36), for $p_1(x)$ we then have

$$0 = Np(x)Q^{N-1}(x)(K-N) - p(x)(K-1)N + K(N-1) .$$

Using $p(x) = -\frac{\partial Q(x)}{\partial x}$ we obtain

$$0 = N(N-K) \frac{\partial Q(x)}{\partial x} Q^{N-1} + (K-1)N \frac{\partial Q(x)}{\partial x} + K(N-1)$$

$$0 = N(N-K) Q^{N-1} dQ + (K-1)N dQ + K(N-1) dx .$$

We can integrate this last expression with respect to x ,

$$0 = (N-K)Q^N(x) + (K-1)NQ(x) + K(N-1)(x-1) , \quad (5.38)$$

where we took care of the boundary condition $Q(1) = 0$, $Q(0) = 1$.

Solution in the Thermodynamic Limit The polynomial Eq. (5.38) simplifies in the thermodynamic limit, with $N \rightarrow \infty$ and $K/N \rightarrow 0$, to

$$0 = Q^N(x) + (K-1)Q(x) - K(1-x) . \quad (5.39)$$

We note that $Q(x) \in [0, 1]$ and that $Q(0) = 1$, $Q(1) = 0$. There must therefore be some $x \in]0, 1[$ for which $0 < Q(x) < 1$. Then

$$Q^N(x) \rightarrow 0, \quad Q(x) \approx \frac{K}{K-1}(1-x) . \quad (5.40)$$

Equation (5.40) remains valid as long as $Q < 1$, or $x > x_c$:

$$1 = \frac{K}{K-1}(1-x_c), \quad x_c = \frac{1}{K} .$$

We then have in the limit $N \rightarrow \infty$

$$\lim_{N \rightarrow \infty} Q(x) = \begin{cases} 1 & \text{for } x < 1/K \\ (1-x)K/(K-1) & \text{for } x > 1/K \end{cases} , \quad (5.41)$$

compare Fig. 5.15, and, using $p(x) = -\partial Q(x)/\partial x$,

$$\lim_{N \rightarrow \infty} p(x) = \begin{cases} 0 & \text{for } x < 1/K \\ K/(K-1) & \text{for } x > 1/K \end{cases} . \quad (5.42)$$

This result compares qualitatively well with the numerical results presented in Fig. 5.14. Note, however, that the mean-field solution Eq. (5.42) does not

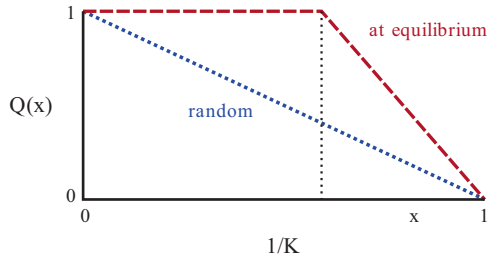


Fig. 5.15 The distribution $Q(x)$ to find a fitness barrier larger than $x \in [0, 1]$ for the Bak and Sneppen model, for the case of random barrier distribution (*dashed line*) and the stationary distribution (*dashed-dotted line*), compare Eq. (5.41)

predict the exact critical barrier height, which is somewhat larger for $K = 2$ and a one-dimensional arrangement of neighbors, as in Fig. 5.14.

1/N Corrections Equation (5.42) cannot be rigorously true for $N < \infty$, since there is a finite probability for barriers with $B_i < 1/K$ to reappear at every step. One can expand the solution of the self-consistency Eq. (5.38) in powers of $1/N$. One finds

$$p(x) \simeq \begin{cases} K/N & \text{for } x < 1/K \\ K/(K-1) & \text{for } x > 1/K \end{cases} . \quad (5.43)$$

We leave the derivation as an exercise for the reader.

Distribution of the Lowest Barrier If the barrier distribution is zero below the self-organized threshold $x_c = 1/K$ and constant above, then the lowest barrier must be below x_c with equal probability:

$$p_1(x) \rightarrow \begin{cases} K & \text{for } x < 1/K \\ 0 & \text{for } x > 1/K \end{cases} , \quad \int_0^1 dx p_1(x) = 1 . \quad (5.44)$$

Equations (5.44) and (5.36) are consistent with Eq. (5.43) for $x < 1/K$.

Coevolution and Avalanches When the species with the lowest barrier mutates we assign new random barrier heights to it and to its $K - 1$ neighbors. This causes an avalanche of evolutionary adaptations whenever one of the new barriers becomes the new lowest fitness barrier. One calls this phenomenon “coevolution” since the evolution of one species drives the adaption of other species belonging to the same ecosystem. We will discuss this and other aspects of evolution in more detail in Chap. ?? . In Fig. 5.16 this process is illustrated for the one-dimensional model. The avalanches in the system are clearly visible and well separated in time. In between the individual avalanches the barrier distribution does not change appreciably; one speaks of a “punctuated equilibrium”.

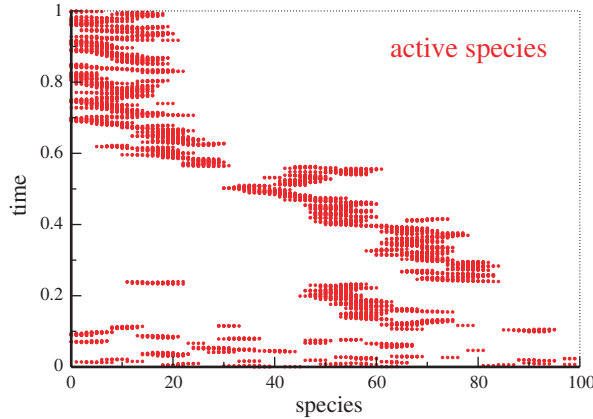


Fig. 5.16 A time series of evolutionary activity in a simulation of the one-dimensional Bak–Sneppen model with $K = 2$ showing coevolutionary avalanches interrupting the punctuated equilibrium. Each *dot* represents the action of choosing a new barrier value for one species

Critical Coevolutionary Avalanches In Sect. 5.5 we discussed the connection between avalanches and random branching. The branching process is critical when it goes on with a probability of $1/2$. To see whether the coevolutionary avalanches within the Bak and Sneppen model are critical we calculate the probability p_{bran} that at least one of the K new, randomly selected, fitness barriers will be the new lowest barrier.

With probability x one of the new random barriers is in $[0, x]$ and below the actual lowest barrier, which is distributed with $p_1(x)$, see Eq. (5.44). We then have

$$p_{\text{bran}} = K \int_0^1 p_1(x) x \, dx = K \int_0^{1/K} K x \, dx = \frac{K^2}{2} x^2 \Big|_0^{1/K} \equiv \frac{1}{2},$$

viz the avalanches are critical. The distribution of the size s of the coevolutionary avalanches is then

$$D(s) \sim \left(\frac{1}{s}\right)^{3/2},$$

as evaluated within the random branching approximation, see Eq. (5.28), and independent of K . The size of a coevolutionary avalanche can be arbitrarily large and involve, in extremis, a finite fraction of the ecosystem, compare Fig. 5.16.

Features of the Critical State The sandpile model evolves into a critical state under the influence of an external driving, when adding one grain of sand after another. The critical state is characterized by a distribution of

slopes (or heights) z_i , one of its characteristics being a discontinuity; there is a finite fraction of slopes with $z_i = Z - 1$, but no slope with $z_i = Z$, apart from some of the sites participating in an avalanche.

In the Bak and Sneppen model the same process occurs, but without external drivings. At criticality the barrier distribution $p(x) = \partial Q(x)/\partial x$ has a discontinuity at $x_c = 1/K$, see Fig. 5.15. One could say, *cum grano salis*, that the system has developed an “internal phase transition”, namely a transition in the barrier distribution $p(x)$, an internal variable. This emergent state for $p(x)$ is a many-body or collective effect, since it results from the mutual reciprocal interactions of the species participating in the formation of the ecosystem.

Exercises

SOLUTIONS OF THE LANDAU–GINZBURG FUNCTIONAL

Determine the order parameter for $h \neq 0$ via Eq. (5.9) and Fig. 5.2. Discuss the local stability condition Eq. (5.3) for the three possible solutions and their global stability. Note that $F = fV$, where F is the free energy, f the free energy density and V the volume.

ENTROPY AND SPECIFIC HEAT WITHIN THE LANDAU MODEL

Determine the entropy $S(T) = \frac{\partial F}{\partial T}$ and the specific heat $c_V = T \frac{\partial S}{\partial T}$ within the Landau–Ginzburg theory Eq. (5.1) for phase transitions.

THE GAME OF LIFE

Consider the evolution of the following states, see Fig. 5.5, under the rules for Conway’s game of life:

$$\{(0,0), (1,0), (0,1), (1,1)\}$$

$$\{(0,-1), (0,0), (0,1)\}$$

$$\{(0,0), (0,1), (1,0), (-1,0), (0,-1)\}$$

$$\{(0,0), (0,1), (0,2), (1,2), (2,1)\}$$

The predictions can be checked with Java-applets you may easily find in the Internet.

THE GAME OF LIFE ON A SMALL-WORLD NETWORK

Write a program to simulate the game of life on a 2D lattice. Consider this lattice as a network with every site having edges to its eight neighbors. Rewire the network such that (a) the local connectivities $z_i \equiv 8$ are retained for every site and (b) a small-world network is obtained. This can be achieved by cutting two arbitrary links with probability p and rewiring the four resulting stubs randomly.

Define an appropriate dynamical order parameter and characterize the changes as a function of the rewiring probability. Compare Chap. ??.

THE FOREST FIRE MODEL

Develop a mean-field theory for the forest fire model by introducing appropriate probabilities to find cells with trees, fires and ashes. Find the critical number of nearest neighbors Z for fires to continue burning.

THE REALISTIC SANDPILE MODEL

Propose a cellular automata model that simulates the physics of real-world sandpiles somewhat more realistically than the BTW model. The cell values $z(x, y)$ should correspond to the local height of the sand. Write a program to simulate the model.

RECURSION RELATION FOR AVALANCHE SIZES

Use the definition (5.22) for the generating functional $f_n(x, p)$ of avalanche sizes in (5.24) and derive a recursion relation for the probability $P_s(n, p)$ of finding an avalanche of size s in the n th generation, given a branching probability p . How does this recursion relation change when the branching is not binary but, as illustrated in Fig. 5.12, determined by the probability p_m of generating m offsprings?

THE RANDOM BRANCHING MODEL

Derive the distribution of avalanche durations Eq. (5.29) in analogy to the steps explained in Sect. 5.5, by considering a recursion relation for the integrated duration probability $\tilde{Q}_n = \sum_{n'=0}^n Q_n(0, p)$, viz for the probability that an avalanche last maximally n time steps.

THE GALTON-WATSON PROCESS

Use the fixpoint condition, Eq. (5.32) and show that the extinction probability is unity if the average reproduction rate is smaller than one.

Further Reading

Introductory texts to cellular automata and to the game of life are Wolfram (1986), Creutz (1997) and Berlekamp et al. (1982). For a review of the forest fire and several related models, see Clar et al. (1996), for a review on absorbing phase transitions Hinrichsen (2000); for a review of sandpiles, see Creutz (2004), and for a general review of self-organized criticality, see Marković et al. (2014). Exemplary textbooks on statistical physics and phase transitions have been written by Callen (1985) and Goldenfeld (1992).

Some general features of $1/f$ noise are discussed by Press (1978); its possible relation to self-organized criticality has been postulated by Bak et al. (1987). The formulation of the Bak and Sneppen (1993) model for long-term coevolutionary processes and its mean-field solution are discussed by Flyvbjerg et al. (1993).

The interested reader may also glance at some original research literature, such as a numerical study of the sandpile model (Prietzhev et al. 1996) and the application of random branching theory to the sandpile model (Zapperi et al. 1995). The connection of self-organized criticality to local conservation

rules is worked out by [Tsuchiya and Katori \(2000\)](#), and the forest fire model with lightning is introduced by [Drossel and Schwabl \(1992\)](#).

References

- BAK, P., SNEPPEN, K. 1993 Punctuated equilibrium and criticality in a simple model of evolution. *Physical Review Letters* **71**, 4083–4086.
- BAK, P., TANG, C., WIESENFIELD, K. 1987 Self-organized criticality: an explanation of $1/f$ noise. *Physical Review Letters* **59**, 381–384.
- BERLEKAMP, E., CONWAY, J., GUY, R. 1982 *Winning Ways for Your Mathematical Plays, Vol. 2*. Academic Press, New York.
- CALLEN, H.B. 1985 *Thermodynamics and Introduction to Thermostatistics*. Wiley, New York.
- CLAR, S., DROSSEL, B., SCHWABL, F. 1996 Forest fires and other examples of self-organized criticality. *Journal of Physics: Condensed Matter* **8**, 6803–6824.
- CREUTZ, M. 1997 Cellular automata and self-organized criticality. In Bhanot, G., Chen, S., Seiden, P. (eds.), *Some New Directions in Science on Computers*, pp. 147–169. World Scientific, Singapore.
- CREUTZ, M. 2004 Playing with sandpiles. *Physica A* **340**, 521–526.
- DROSSEL, B., SCHWABL, F. 1992 Self-organized critical forest-fire model. *Physical Review Letters* **69**, 1629–1632.
- FLYVBJERG, H., SNEPPEN, K., BAK, P. 1993 Mean field theory for a simple model of evolution. *Physical Review Letters* **71**, 4087–4090.
- GOLDENFELD, N. 1992 *Lectures on Phase Transitions and the Renormalization Group*. Perseus Publishing, Reading, MA.
- HINRICHSSEN, H. 1993 Non-equilibrium critical phenomena and phase transitions into absorbing states. *Advances in Physics* **49**, 815–958.
- MARKOVIĆ, D., GROS, C. 2014 Powerlaws and Self-Organized Criticality in Theory and Nature. *Physics Reports* **536**, 41–74.
- PRESS, W.H. 1978 Flicker noises in astronomy and elsewhere. *Comments on Modern Physics, Part C* **7**, 103–119.
- PRIEZZHEV, V.B., KSTITAREV, D.V., IVASHKEVICH, E.V. 1996 Formation of avalanches and critical exponents in an abelian sandpile model. *Physical Review Letters* **76**, 2093–2096.
- TSUCHIYA, T., KATORI, M. 2000 Proof of breaking of self-organized criticality in a non-conservative abelian sandpile model. *Physical Review Letters* **61**, 1183–1186.
- WOLFRAM, S. (ED.). 1986 *Theory and Applications of Cellular Automata*. World Scientific, Singapore.
- ZAPPERI, S., LAURITSEN, K.B., STANLEY, H.E. 1995 Self-organized branching processes: Mean-field theory for avalanches. *Physical Review Letters* **75**, 4071–4074.